Forest fire detection based on temporal and spatial correction of background brightness temperature using GF-4 PMI data

Peng Cheng[1], Haigang Sui[1,]*, Jianxun Wang[1], Li Hua[3], Junyi Liu[1], Qiming Zhou[2], Yong Zeng[4]

[1]State Key Laboratory of Information Engineering in Surveying Mapping and Remote Sensing, Wuhan University, Wuhan 430079, China.
[2]Institute of Research and Continuing Education (IRACE), Hong Kong Baptist University, Hong Kong.
[3]College of Resources and Environment, Huazhong Agricultural University, Wuhan 430079, China.
[4]China Centre for Resources Satellite Data and Application (CRESDA), Beijing 100094, China.

Keywords: Wildfire detection, GF-4, Brightness temperature correction, dynamic threshold.

Abstract

Forest fires threaten human life and property, making timely and accurate fire monitoring essential for fire prevention and control efforts. Satellite remote sensing meets the requirements of large-scale, high-frequency observations for forest fire monitoring and has been widely applied in this field. Chinese Gaofen-4 (GF-4) satellite, a geostationary satellite equipped with a mid-infrared sensor, holds significant potential for forest fire monitoring. However, existing fire detection methods for GF-4 data, which use fixed initial thresholds and insufficiently account for the influence of fires on background brightness temperatures, often result in high rates of false positives and missed detections. To maximize the application potential of GF-4 data in forest fire monitoring and improve the accuracy of fire detection, this study proposes a novel fire detection method based on spatiotemporal correction of background brightness temperature, tailored to the characteristics of GF-4 PMI data and incorporating a contextual fire detection approach within the infrared spectrum. In this method, dynamic thresholds based on brightness temperature distributions are employed to extract potential fire points, and the background brightness temperature is corrected by utilizing imagery from the same time on the previous day and the brightness temperature from the outer edges of the background window, thereby reducing fire effects on background temperatures. Final fire detection is achieved by distinguishing potential fire points based on the difference between the brightness temperatures of potential fire points and the corrected background, effectively filtering false positives. In case studies of two fires in Ganzi Tibetan Autonomous Prefecture, Sichuan Province, and Chongqing, China, visually interpreted fire detection results were used as references. The proposed method significantly reduced false and missed detections compared to traditional contextual threshold methods. It achieved an overall evaluation index exceeding 0.81, demonstrating high reliability and applicability for forest fire detection and extraction using GF-4 PMI imagery.

1. Introduction

Forests play a crucial role in conserving soil and water resources and regulating climate, making them an indispensable component of ecosystems (Wingfield et al., 2015). However, with the increasing frequency of global forest fires, forests, human life, and property face serious wildfire threats (Rashkovetsky et al., 2021). Detecting fires accurately and promptly allows for implementing fire prevention and suppression measures before they develop into large-scale wildfires. This effectively reduces firefighting difficulty and minimizes losses. Unfortunately, large parts of forest areas are rarely visited by humans, and the occurrence of fires is often highly random. Hence, they are usually only observed when the fire has spread to a large area, making it very difficult to control and extinguish (Alkhatib, 2014). With its extensive monitoring range and high observation frequency, satellite remote sensing can detect forest fires promptly and has been widely applied in forest fire monitoring (Barmpoutis et al., 2020).

Forest fires are intense, anomalous disturbances within a relatively homogeneous forest background. Under normal conditions, forest radiation represents background radiation; However, the flame, smoke, and other by-products generated during the fire show special radiation characteristics. These special emissions stand out as anomalous disturbances against the background radiation, enabling satellite detection of forest fires primarily by identifying the radiative differences between fire-affected areas and their surroundings. Compared to other radiative characteristics, thermal anomaly is a typical characteristic of forest fires. According to Planck's law and Wien's displacement law, as temperature increases, the peak wavelength of blackbody radiation shifts toward shorter wavelengths. Forest fire temperatures typically range from 500 to 800 K, with maximum radiative energy occurring within the 3–5μm wavelength range. In lower-temperature fire regions, the peak radiative wavelength lies in the thermal infrared range (approximately 10μm). This forms the theoretical foundation for forest fire monitoring using mid-infrared and thermal infrared bands (Giglio et al., 2003). However, due to limitations in infrared sensing technology, some moderate-resolution and high-resolution multispectral satellites lack mid-wave infrared bands and thermal-infrared bands, though most include at least one short-wave infrared band (with a central wavelength of 1.64μm or 2.2μm). Given the proximity of the short-wave infrared range to the mid-infrared, it remains relatively sensitive to high-temperature targets, such as fires, making it feasible to monitor forest fires by combining near-infrared and visible data (Schroeder et al., 2016).

Based on the above theory, the mainstream method for satellite-based fire detection involves identifying infrared radiation anomalies to detect forest fires. Various forest fire detection methods have been developed, tailored to the specific characteristics of different satellite sensors. Moderate-to-low spatial resolution satellites have shorter revisit periods and can monitor forest fires frequently, enabling the timely

https://doi.org/10.5194/isprs-annals-X-G-2025-189-2025

identification of fire anomalies. For example, the brightness temperature threshold method applied to NOAA satellite data uses the temperature difference in Channel 3 to extract forest fires, with smoke and other auxiliary information added to enhance detection accuracy (Flasse et al., 1996; Kawano et al., 1999). However, the threshold method suffers from poor regional adaptability, often resulting in false positives and missed detections. Consequently, Kudoh et al. developed a method that combines brightness temperature with a normalized vegetation index by constructing normalized difference near-infrared and visible-near-infrared indices, significantly improving fire detection accuracy (Kudoh et al., 1999). Nevertheless, regional and seasonal factors can still affect detection accuracy, leading to the proposal of a contextual fire point algorithm with neighborhood analysis to further enhance detection capabilities (Nakayama, 1999). Himawari-8 satellite data is also widely used for fire monitoring; the main methods include the adaptive threshold fire detection algorithm (Chen et al., 2017) and the sequential fire detection method (Chen et al., 2021), which have demonstrated good results.

MODIS data are the most widely used for satellite fire monitoring, and various fire detection algorithms have been developed for this data. These include an adaptive fire point monitoring algorithm that automatically derives fire point thresholds using histograms (He et al., 2007), a three-channel enhancement algorithm combined with smoke feature recognition (Huang et al., 2007), and a complementary color method for highlighting fire points visually (Zhaxi et al., 2010), all of which have shown effectiveness in practical applications. However, the most classic method for MODIS data is the contextual threshold algorithm proposed by Giglio, which masks cloud and water pixels, sets a background window based on radiative brightness temperature, and statistically characterizes brightness temperature features within the window. Fire points are then identified based on the temperature difference between the central pixel and the background. This approach significantly reduces false positives and improves detection accuracy, making it widely used in MODIS fire detection applications (Giglio et al., 2003). To address the misclassification of bare ground and small water bodies as fire points, this method was later enhanced with additional discriminators for coastal pixels, forest bare ground, and small water bodies, further reducing false positives and enabling the detection of forest fires as small as 100 m^2 (Giglio et al., 2016). After over 20 years of research and application, MODIS data has become a critical source for operational forest fire monitoring, providing crucial support for early fire detection, assessment of fire progression, and firefighting efforts.

Medium-to-low resolution satellite data are characterized by short revisit cycles but lower resolution, making them less effective for monitoring small fires than high-resolution satellites. Fire detection methods utilizing Landsat satellite data, such as the Normalized Difference Fire Index (NDFI) (Zhu et al., 2011) and the Normalized Burn Ratio (NBR) threshold method (He et al., 2016), can detect forest fires as small as 4 m^2 under ideal conditions, providing much higher detection sensitivity than medium-to-low resolution satellites. However, due to their longer revisit periods, these satellites are less effective for the timely detection of fires. With the full-scale launch of the Chinese "High-Resolution Earth Observation Program," the Gaofen satellite series has provided abundant data for disaster monitoring. Among them, the Gaofen-4 (GF-4) satellite, a geostationary satellite with key technical specifications shown in Table 1, is equipped with visible, near-infrared, and mid-infrared sensors. It can observe with a revisit cycle of 20 seconds, showing great potential for applications in thermal anomaly and forest fire monitoring. Using GF-4 data, the split-window method constructs adaptive thresholds for fire detection, achieving an accuracy rate above 80%; however, it still suffers from a relatively high rate of missed detections (Liu et al., 2020). A fire detection method using two images to correct brightness temperature differences has been proposed to address the issue of high missed detection rates, further improving the accuracy of fire detection (Wang et al., 2021). In summary, various satellite data, supported by corresponding algorithms, can effectively detect forest fires but still face false and missed detections of smaller fire points. GF-4, with its 400-meter resolution mid-infrared sensor and geostationary orbit, has significant untapped potential for fire monitoring.

To enhance GF-4's fire monitoring capabilities, this study proposes a dynamically initialized contextual threshold method combined with spatiotemporal correction of background brightness temperature. The traditional contextual threshold method identifies potential fire points using a fixed threshold. Then, it verifies real fire points by comparing the brightness temperature of potential fire points with the average brightness temperature of surrounding pixels (background brightness temperature). Our approach, based on the classic contextual threshold method, dynamically adjusts the threshold for potential fire points based on the distribution of brightness temperatures in the image, reducing the probability of missing detection of small fire points in low-temperature areas. Additionally, the background brightness temperature of potential fire points is corrected spatiotemporally using imagery from the same location and time on the previous day, avoiding interference from fires on background brightness temperature, which could otherwise impair accurate fire point identification.

The primary contributions of this study are as follows:

(1) We propose an innovative fire detection method using a dynamically initialized contextual threshold with spatiotemporal correction of background brightness temperature. This method considers the influence of potential fire points in low-temperature regions and fire effects on background brightness, aiming to reduce the rates of missed small fires and false positives in GF-4's forest fire monitoring.

(2) To better adapt to global brightness temperature variations across different regions and seasons, a dynamic initial threshold is introduced. This allows for initial threshold adjustment based on the brightness temperature distribution in the image, effectively reducing the probability of missed detections for small fires.

(3) To mitigate the effect of fires on background brightness temperature, we correct the current background brightness temperature using brightness data from imagery taken at the same time and location on the previous day, making it closer to the true background temperature in non-fire conditions. This approach enhances fire detection capability and reduces false positives.

Table 1. Payload technical index of GF-4 satellite

Payload	Spectral number	Spectral range/μm	Spatial resolution/m	Swath width/km	Revisit time/s
Panchromatic multispectral camera (PMS)	1	0.45—0.90	50	>400	20
	2	0.45—0.52	50	>400	20
	3	0.52—0.59	50	>400	20
	4	0.63—0.69	50	>400	20
	5	0.77—0.89	50	>400	20
Intermediate infrared camera (IRS)	6	3.50—4.10	400	>400	20

https://doi.org/10.5194/isprs-annals-X-G-2025-189-2025 |

2. Methodology

2.1 Overview

The workflow of the dynamically initialized contextual threshold method with spatio-temporal correction of background brightness temperature is illustrated in Figure 1. After acquiring the GF-4 imagery, the process begins with pre-processing to obtain corrected multispectral and infrared brightness temperature images. Cloud and water masks are applied using multispectral imagery. Then, non-forest areas are masked out based on pre-disaster, preprocessed multi-band imagery. An initial threshold is used to classify the remaining pixels into potential fire pixels and non-fire pixels. For each potential fire pixel, background brightness temperature correction is applied using supplementary imagery, then the brightness temperature difference between potential fire pixels and their corrected background brightness is calculated. This difference is used to identify fire pixels.

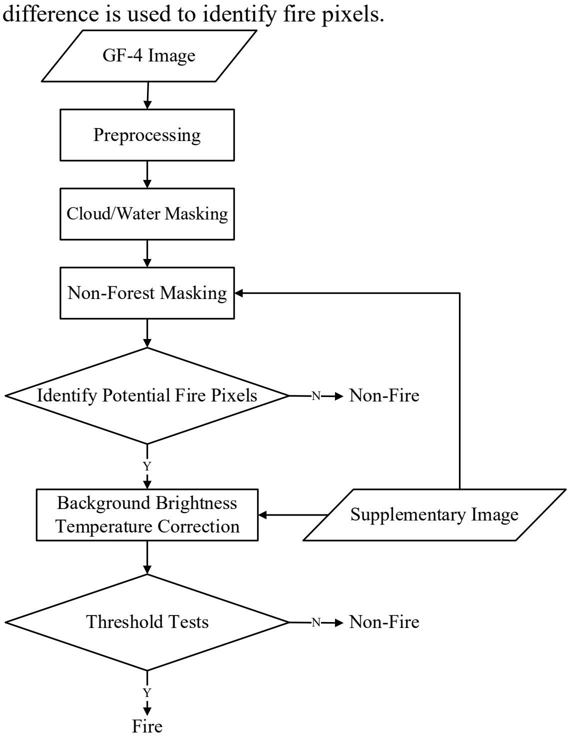

Figure 1. Flowchart of Fire Point Detection Method

2.2 Image preprocessing

The raw satellite imagery, having undergone only basic pre-processing, cannot be directly used for fire detection. The selected GF-4 PMI imagery requires additional processing, including radiometric calibration, geometric correction, brightness temperature retrieval, and reflectance calculation. First, radiometric calibration is applied to the GF-4 imagery to compute the apparent radiance. Based on DEM data, geometric correction is performed on the apparent radiance images. Subsequently, the apparent radiance of the panchromatic and multispectral bands is converted to apparent reflectance, while that of the mid-wave infrared is converted to brightness temperature. Finally, the panchromatic, multispectral, and near-infrared bands with 50-meter resolution are resampled to a spatial resolution of 400 m. These resampled bands are combined with the brightness temperature data derived from the mid-wave infrared to create a new, restructured image file.

2.3 Mask processing

Forest fire monitoring primarily targets forest and grassland areas, while cloud pixels and water bodies can interfere with fire detection. Therefore, non-forest areas, clouds, and water are masked in the pre-processed images. Cloud pixels are identified and masked using a combination of formulas (1) and (2) (Liu et al., 2019).

$$\rho_4 + \rho_5 > 0.7 \tag{1}$$

$$T < 285K \tag{2}$$

Where ρ_4 and ρ_5 represent the reflectance values for the 4th band (red) and 5th band (near-infrared) of the PMS sensor, respectively, T denotes the mid-infrared brightness temperature of the IRS sensor.

For water body masking, water pixels are identified using formulas (3) and (4) (Xu Hanqiu, 2005).

$$\mathrm{NDWI} = \frac{\rho_3 - \rho_5}{\rho_3 + \rho_5} > 0.1 \tag{3}$$

$$\rho_5 < 0.17 \tag{4}$$

Here, ρ_3 represents the reflectance of the 3rd band (green) of the PMS sensor.

Based on supplementary imagery before the disaster, the Normalized Difference Vegetation Index (NDVI) is calculated using formula (5) to extract forest and grassland areas. Non-forest and non-grassland regions within the target imagery are masked, resulting in an image that retains only forested and grassland areas for fire detection (Carlson and Ripley, 1997).

$$\mathrm{ND}VI = \frac{\rho_5 - \rho_4}{\rho_4 + \rho_5} > 0.2 \tag{5}$$

2.4 Potential fire point identification

Traditional methods determine a fixed initial threshold for potential fire pixel extraction based on experimental or empirical values. If the threshold is too high, low-temperature fire points or fires in generally low-temperature regions during the early burning stages are likely to be missed. Conversely, if the threshold is too low, it can identify numerous potential fire points, increasing false detections and reducing detection efficiency. Additionally, a fixed threshold struggles to adapt to the dynamic temperature changes across regions and seasons due to seasonal and topographic variations. Therefore, this study proposes a dynamic initial threshold based on the brightness temperature distribution of the target imagery, using formula (6) to extract potential fire points.

$$\begin{cases} T > MIN\{T_{2\%},\ 315K\} \\ T > 290K \end{cases} \tag{6}$$

Here, T represents the mid-infrared brightness temperature from the IRS sensor and $T_{2\%}$ denotes the 2% lower boundary value of the brightness temperature distribution in the target image.

https://doi.org/10.5194/isprs-annals-X-G-2025-189-2025

2.5 Background brightness temperature spatiotemporal correction

Further confirmation of potential fire pixels is achieved by evaluating the difference between each potential fire pixel's brightness temperature and its surrounding pixels' average brightness temperature (background brightness). The background brightness is calculated within a window centered on the potential fire pixel, where all valid pixels, excluding the central pixel, are averaged. Valid pixels exclude missing pixels, other potential fire pixels, clouds, and water bodies. If the count of valid pixels is less than 25% of the total number in the window, the window size expands from 3×3 to 5×5, with a maximum limit of 27×27.

Since the background brightness may be elevated by the influence of the central fire, potentially reducing the temperature difference between the central pixel and its background and causing fire misclassification, this study introduces a spatiotemporal correction for background brightness. The concept is based on the limited spatial influence of fire on surrounding pixels (Tang et al., 2020). After determining the background window, an expanded ring of two pixels surrounding this window is averaged to derive an "expanded brightness," which is assumed to be minimally affected by the fire and thus represents unaffected brightness. Furthermore, under normal conditions, the temperature difference between adjacent areas does not vary significantly over consecutive days at the same time (Han et al., 2013). Therefore, the difference between the expanded brightness and the background brightness in the image from the same time on the previous day is assumed to be equal to the difference between the expanded brightness and the unaffected background brightness in the current image. The background brightness temperature not affected by the fire can be obtained according to the extended brightness temperature of the image to be detected and the difference between the previous day's extended brightness temperature and the background brightness temperature. Ensuring that only valid pixels are included in the calculation.

As shown in Figure 2, the red rectangular box indicates the selected window, with yellow squares representing background pixels. M_1 and M_0 correspond to the background brightness temperatures for the target image and the image from 24 hours prior, respectively. Blue squares represent expanded pixels, with E_1 and E_0 representing the expanded brightness temperatures for the current and prior images, respectively. d denotes the difference between E_0 and M_0.

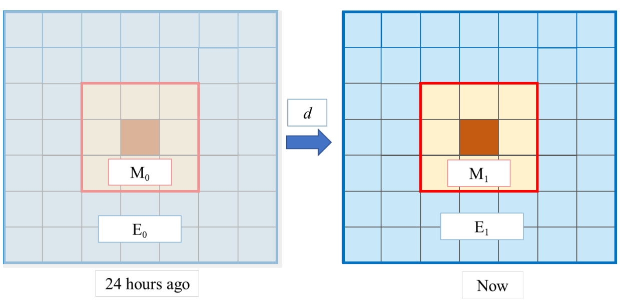

Figure 2. Schematic diagram of background brightness temperature and extended brightness temperature

According to equation (7), the background brightness temperature unaffected by the fire can be calculated.

$$M = E_1 - d \tag{7}$$

Where M is the background brightness temperature, which is not affected by the fire. If the center pixel of the image 24 hours ago was a fire pixel, no background brightness temperature correction will be performed.

2.6 Fire detection

A potential fire pixel is classified as a fire pixel if it satisfies formula (8).

$$T_1 - M > MAX\{10K, 3\delta\} \tag{8}$$

Where T_1 represents the brightness temperature of the potential fire pixel, and δ denotes the standard deviation of the background pixel brightness temperatures within the target image window.

2.7 Accuracy evaluation method

The accuracy evaluation is conducted by comparing the true values with the detection results obtained by the algorithm, utilizing precision (P), missed detection rate (M), and comprehensive evaluation index (F) to assess the accuracy of the detection method. The calculations of P, M, and F are shown in equations (9) to (11) respectively (He et al., 2016).

$$P = Y_y/(Y_y + Y_N) \tag{9}$$

$$M = N_y/(Y_y + N_y) \tag{10}$$

$$F = \frac{2\times P\times(1-M)}{1+P-M} \tag{11}$$

Where Y_y represents the number of pixels detected as real fire points by the algorithm, Y_N represents the number of pixels erroneously detected as fire points by the algorithm, N_y represents the number of fire point pixels missed by the algorithm, P represents the accuracy rate, M represents the missed detection rate, and F represents the comprehensive evaluation index.

3. Experimental results and analysis

3.1 Data and experiments

To evaluate the effectiveness of this fire detection method, two fire cases were selected: the forest fire in Ganzi Tibetan Autonomous Prefecture, Sichuan Province, on March 14, 2024, and the forest fire in Chongqing, China, on August 22, 2022. Detailed information on the experimental data is provided in Table 2. Data processing for these experiments follows the steps outlined in Section 2, with preprocessing steps in Sections 2.2 to 2.3 performed using ENVI 5.3 and fire point extraction in Sections 2.4 to 2.5 completed with a Python-based algorithm. During the image processing process, to better demonstrate the effectiveness of fire point extraction, the original image was tailored accordingly based on the distribution range of fire points in each case after preprocessing the original image. To better assess the experimental results, the traditional contextual threshold method was used for comparison. This conventional method has a similar workflow to that in Figure 1. Still, it uses a fixed threshold of 315K for potential fire point identification

https://doi.org/10.5194/isprs-annals-X-G-2025-189-2025

and does not apply corrections to background brightness temperature.

Table 2. Details of GF-4 satellite data

Experimental Area	Time of fire detection image	Time of Supplementary image	Image type
Ganzi Tibetan Autonomous Prefecture,	2024-03-17 01:00:21	2024-03-16 01:00:21	PMI
Chongqing,	2022-08-22 02:48:34	2022-08-21 02:48:34	PMI

3.2 Results

This experiment used the spatiotemporal background brightness temperature correction method and the traditional contextual threshold method to extract fire points. Due to the lack of higher spatial resolution satellite imagery and ground truth data for forest fires in the experimental areas, the fire points interpreted visually from the fire detection imagery are taken as the ground truth in this study. The extraction results for the forest fire in Garze Tibetan Autonomous Prefecture, Sichuan Province, on March 14, 2024, are shown in Figure 3. In the figure, red pixels represent fire points; Figure 3(a) shows the visual interpretation result, with an RGB composite image using bands 4, 3, and 2 as the background; Figure 3(b) displays the same visual interpretation result as in Figure 3(a) but with a brightness temperature image as the background. Figures 3(c) and 3(d) show the extraction results from the traditional contextual threshold and proposed methods, respectively, with RGB imagery as the background. In this fire case, 55 fire pixels were visually interpreted, while the traditional contextual threshold method extracted 9 fire pixels, and the background brightness temperature correction method extracted 48 fire pixels.

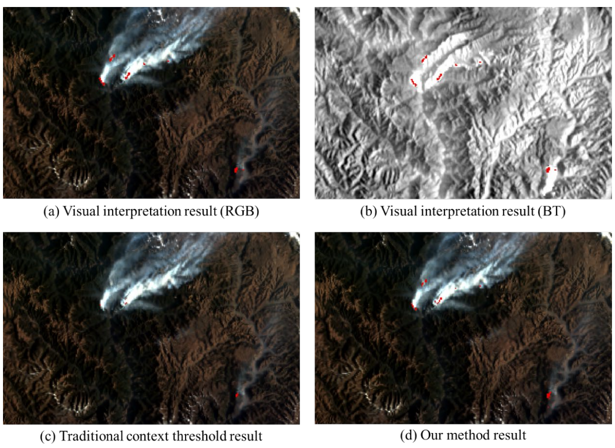

Figure 3. Forest fire extraction results in Ganzi Tibetan Autonomous Prefecture, Sichuan Province

The extraction results for the forest fire in Chongqing, China, on August 22, 2022, are shown in Figure 4. In the figure, red pixels represent fire points. Figure 4(a) displays the visual interpretation result, with an RGB composite image using bands 4, 3, and 2 as the background; Figure 4(b) shows the same visual interpretation result as in Figure 4(a) but with a brightness temperature image as the background. Figures 4(c) and 4(d) show the extraction results using the traditional contextual threshold and proposed methods, respectively, with the RGB image as the background. In this fire case, 44 fire pixels were visually interpreted, while the traditional contextual threshold method extracted 28 fire pixels, and the background brightness temperature correction method extracted 39 fire pixels.

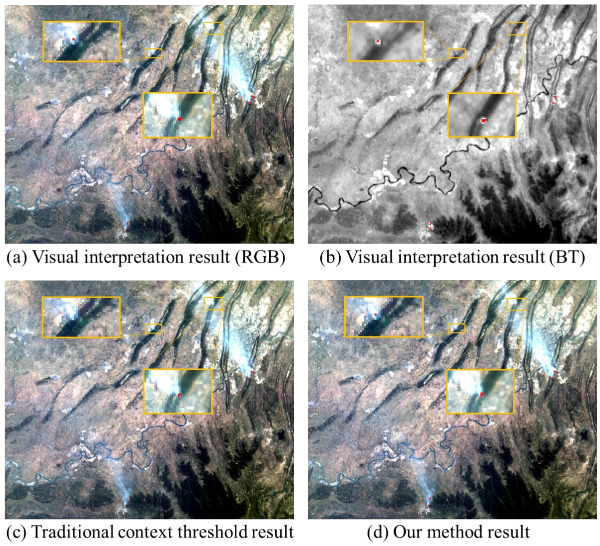

Figure 4. Forest fire extraction results in Chongqing, China

3.3 Accuracy verification and analysis

The detailed results for the forest fire case in Garze Tibetan Autonomous Prefecture, Sichuan Province, on March 14, 2024, are shown in Table 3. While the traditional contextual threshold method achieved a high accuracy of 100%, it had an extremely high omission rate. This is likely because the fire occurred in winter, when temperatures were relatively low, making it challenging for a fixed threshold to detect relatively low-temperature fire points, leading to numerous omissions. In contrast, the spatiotemporal correction method based on background brightness temperature can dynamically adjust according to the overall brightness temperature distribution. This method's initial threshold for this case was significantly lower than the fixed threshold, substantially reducing fire omission rates and achieving a higher overall evaluation score.

Table 3. Fire extraction results of Ganzi Tibetan Autonomous Prefecture

	Potential fire pixels number	Extracted fire pixels number	Extracted real fire pixels number	P↑	M↓	F↑
Tradition-al context threshold method	17	9	9	**1**	0.863	0.241
Our method	76	48	42	0.875	**0.236**	**0.816**

The detailed results for the forest fire case in Chongqing, China, on August 22, 2022, are shown in Table 4. The spatiotemporal correction method based on background brightness temperature outperformed the traditional contextual threshold method in terms of accuracy, omission rate, and overall evaluation metrics. By dynamically lowering the initial threshold to reduce omissions and applying background brightness temperature corrections, this method enabled more accurate identification of potential fire points, increasing detection accuracy and reducing false detections.

Table 4. Fire extraction results of Chongqing City

	Potential fire pixels number	Extracted fire pixels number	Extracted real fire pixels number	P ↑	M ↓	F ↑
Tradition-al context threshold method	42	28	25	0.893	0.432	0.694
Our method	164	39	37	**0.949**	**0.159**	**0.892**

Analyzing the fire point detection results from the two experimental cases and the two methods, it was found that the fire point extraction methods based on mid-infrared information could effectively capture fire data; however, each had varying degrees of false detections and omissions. Regarding false detections, both the spatiotemporal background brightness temperature correction method and the traditional contextual threshold method had some inaccuracies, likely due to the high-temperature smoke produced by fires.

Both methods also exhibited omissions, which fell into two primary categories: small, isolated fire points and edge pixels of fires. The first type of omission generally occurs when the fire area is small and the temperature is relatively low, resulting in low thermal radiation received by the sensor and, thus, insufficient contrast with the background temperature to be detected. In the Ganzi Tibetan Autonomous Prefecture case, both methods missed small fire points in the southeast of the image; however, in the Chongqing case, our method successfully detected small fire points in the northern region that the traditional contextual threshold method missed, suggesting improved detection of smaller fire points with our approach.

Edge pixel omissions mostly arise from mixed pixels near fire boundaries, where only part of the pixel represents fire, causing a lower brightness temperature while the surrounding pixel temperature is raised due to the fire’s influence. The fixed initial threshold used in the traditional contextual threshold method performed well in the summer Chongqing case but poorly in the winter Ganzi case. While a fixed threshold might work well in specific regions, it struggles with variations due to season, weather, and terrain. Furthermore, the fire’s active burning could have raised background brightness temperatures, decreasing the contrast with potential fire pixels and increasing omissions. However, our method uses a dynamic threshold determined based on brightness temperature distribution, which adapts more effectively to such changes. Feedback from factors affecting brightness temperature distribution is incorporated into the dynamic threshold, making it better suited to the current brightness temperature image and reducing fire omissions. Additionally, our background brightness temperature correction significantly minimizes interference from fire on background temperatures, allowing for more accurate calculation of differences between potential fire pixel temperatures and "true" background temperatures, thus improving detection accuracy and reducing omissions.

Overall, validation results indicated that the spatiotemporal correction method based on background brightness temperature outperformed the traditional contextual threshold method in both cases, showing superior fire extraction effectiveness.

4. Discussion

The experimental cases in this study provide evidence to some extent for the effectiveness and advancement of the spatiotemporal correction method based on background brightness temperature. Fire monitoring using GF-4 satellite data primarily relies on the mid-infrared band, which is also available in MODIS data. Additionally, MODIS has relatively fixed daily imaging times, which satisfy the requirement for background brightness temperature correction using images from the same time on the previous day. Therefore, when applied to fire monitoring with MODIS data, this method is theoretically expected to perform well. The spatiotemporal correction method based on background brightness temperature can also be applied to other satellite datasets with similar conditions. However, due to calibration differences among different sensors, certain parameters in this method need to be adjusted accordingly to accommodate sensor variations.

Due to data availability constraints, this study presents only two representative cases to demonstrate the effectiveness and advancement of the proposed method. Future research will extend the experiments to include scenarios such as dense cloud coverage and diverse forest types to further validate the robustness of the method.t

5. Conclusions

The GF-4 satellite features flexible imaging modes, high resolution, and frequent capture capabilities, providing robust information support for disaster prevention and reduction. Due to the single mid-infrared channel characteristic of GF-4 PMI data, it effectively detects forest fires by utilizing reflectance from the visible and near-infrared bands and brightness temperature information from the mid-infrared band. This study develops a fire detection method incorporating spatiotemporal correction of background brightness temperature pre-disaster data. Fire detection and accuracy evaluation were conducted in two experimental areas, comparing the results with those obtained from the contextual threshold method.

The experimental results demonstrate that the proposed algorithm significantly reduces omissions and false detections compared to the contextual threshold algorithm. It is also less constrained by seasonal, weather, and terrain factors, exhibiting strong stability. This algorithm's fire point detection accuracy exceeds 87%, and the comprehensive evaluation index is above 0.81, confirming that the proposed method can effectively detect fires with high reliability. However, the algorithm faces a challenge with a high false detection rate of fire points under smoky conditions. Future work will focus on optimizing the algorithm to minimize the impact of smoke on fire point detection and improve the threshold selection for brightness temperature differences.

Acknowledgments

This research is supported by the Guangxi Science and Technology Major Project (No. AA22068072), National Natural Science Foundation of China Major Program (42192580, 42192583)

References

Alkhatib, Ahmad A A., 2014. A Review on Forest Fire Detection Techniques. International Journal of Distributed Sensor Networks, 2014: 103-110. DOI: 10.1155/2014/597368.

Barmpoutis P, Papaioannou P, Dimitropoulos K ,et al., 2020. A Review on Early Forest Fire Detection Systems Using Optical Remote Sensing. Sensors (Basel, Switzerland), 20(22). DOI:10.3390/s20226442.

Carlson T., Ripley D A J., 1997. On the Relation between NDVI, Fractional Vegetation Cover, and Leaf Area Index. Remote Sensing of Environment: An Interdisciplinary Journal, DOI:10.1016/S0034-4257(97)00104-1.

Chen Jie, Zheng Wei, Liu Cheng, 2017. Himawari-8 geostationary meteorological satellite grassland fire monitoring and analysis. Journal of Natural Disasters, 26 (04): 197-204.

Chen Jie, Zheng Wei, Liu Cheng, Tang Shihao, 2021. Himawari-8 Geostationary Meteorological Satellite Time Series Method for Fire Point Detection. Journal of Remote Sensing, 25 (10): 2095-2102.

Flasse S P, CECCATO P., 1996. A contextual algorithm for AVHRR fire detection. International Journal of Remote Sensing, 17(2):419-424.

Giglio L, Descloitres J, Justice C O and Kaufman Y J., 2003. An enhanced contextual fire detection algorithm for MODIS. Remote Sensing of Environment, 87(2/3): 273-282.

Han Cuihua, Hao Zhixin, Zheng Jingyun., 2013. Zoning and regional characteristics of temperature change in China from 1951 to 2010. progress in Geographical Sciences, 032 (006): 887-896.

He Quanjun, Liu Cheng., 2008. Improved Algorithm of Self-adaptive Fire Detection for MODIS Data. Journal of Remote Sensing, 448-453. DOI： 10.11834/jrs.20080361.

He Y, Yang J, Ma Y, Liu J B, Chen F, Li X P and Yang Y F., 2016. A method for fire detection using Landsat 8 data. Journal of Infrared and Millimeter Waves, 35(5): 600-608, 624.

He Yang, Yang Jin, Ma Yong et al., 2016. Fire point detection method based on Landsat-8 land satellite data Journal of Infrared and Millimeter Wave, 35 (5): 10.

Huang Chaofa, Liu Jurong., 2007. A Brief Analysis of the Application of MODIS (Terra/Aqua) Data in Forest Fire Monitoring in Fujian Province. Fujian Forestry Science and Technology, 89-92.

Kawano K, Kudoh J, Makino S., 1999. Forest fire detection in Far East Region of Russia by using NOAA AVHRR images. IEEE International Geoscience & Remote Sensing Symposium, Hamburg, Germany, 858- 860.

Kudoh J., 1999. Forest fire detection in Far East Region of Russia with NOAA-15 in 1998. IEEE International Geoscience & RemoteSensing Symposium, Hamburg, Germany,182-184.

Liu S C，Li X T，Qin X L，Sun G F and Liu Q., 2020. Adaptive threshold method for active fire identification based on GF-4 PMI data. Journal of Remote Sensing，24（3）：215-225.

Liu Xinyan, Sun Lin, Yang Yikun et al., 2019. Cloud and Cloud Shadow Detection Algorithm for Gaofen-4 Satellite Data. Acta Optica Sinica, 39(1):0128001. DOI:10.3788/AOS201939.0128001.

Nakayama M., 1999. Contextual algorithm adapted for NOAA-AVHRR fire detection in Indonesia. International Journal of Remote Sensing, 20(17):3415-3421.

Rashkovetsky, D., Mauracher, F., Langer, M., Schmitt, M., 2021. Wildfire detection from multisensor satellite imagery using deep semantic segmentation. IEEE J. Sel. Top. Appl. Earth Obs. Remote Sens. 14, 7001–7016.

Schroeder W., Oliva P., Giglio L., Quayle B., Lorenz E. and Morelli F., 2016. Active fire detection using Landsat-8/OLI data. Remote Sensing of Environment, 185: 210-220.

Tang F., Hu P., Wen J., 2020. Experimental investigation on lateral ceiling temperature distribution induced by wall-attached fire with various burner aspect ratios in underground space. Fire Safety Journal, 103055. DOI:10.1016/j.firesaf.2020.103055.

Wang Yao, Wang Shixin, Zhou Yi, Wang Futao, Wang Zhenqing, 2021. Research on Fire Point Monitoring Based on GaoFen-4 Satellite Data With Bright Temperature Difference Correction. Spectroscopy and Spectral Analysis, 41(11): 3595.

Wingfield, M.J., Brockerhoff, E.G., Wingfield, B.D., Slippers, B., 2015. Planted forest health: the need for a global strategy. Science 349, 832–836.

Xu H Q., 2005. A study on information extraction of water body with the modified normalized difference water index (MNDWI). Journal of Remote Sensing,

Zhaxi Dunzhu, Laba, Wang Caiyun. 2010. The application of EOS/MODIS data supported by 3S in forest fire monitoring in Xizang. Anhui Agricultural Science, 38 (28): 15714-15717.

Zhu Yajing, Xing Lixin, Pan Jun et al., 2011. Research on Short Wave Infrared Remote Sensing High Temperature Land Target Recognition Method Remote Sensing Information, 33-36, 41.